

date: January 15, 2018

to: D. VanGoethem

from: E. Corona

subject: Multilinear stress-strain and failure calibrations for Ti-6Al-4V

Introduction

This memo concerns calibration of an elastic-plastic J_2 material model for Ti-6Al-4V (grade 5) alloy based on tensile uniaxial stress-strain data obtained in the laboratory. In addition, tension tests on notched specimens provided data to calibrate two ductile failure models: Johnson-Cook and Wellman's tearing parameter. The tests were conducted by Kim Haulenbeek and Dave Johnson (1528) in the Structural Mechanics Laboratory (SML) during late March and early April, 2017. The SML EWP number was 4162.

The stock material was a TIMETAL®6-4 Titanium billet with 9 in. by 9 in. square section and length of 137 in. The product description indicates that it was a forging delivered in annealed condition (2 hours @ 1300°F, AC at the mill). The tensile mechanical properties reported in the material certification are given in Table 1, where σ_o represents the 0.2% strain offset yield stress, σ_u the ultimate stress, ε_f the elongation at failure and R.A. the reduction in area.

Table 1. Tensile mechanical properties reported in the material certification.

σ_o	σ_u	ε_f	R.A.
(ksi)	(ksi)	(%)	(%)
132	143	17	34

In addition, the typical elastic properties of this alloy as listed in the Metallic Materials Properties Development and Standardization MMPDS-08 are as follows: Young's modulus, $E = 16.9 \times 10^3$ ksi and Poisson's ratio $\nu = 0.31$.

The specimens used for calibration, however, were not extracted directly from the bar. Instead, the stock was first used to make a hollow male threaded part with circular cross-section for a bending test to simulate a threaded connection subjected to 4-point bending.

The maximum outer diameter of the part was 8.5 in. with a inner diameter of 6.906 in. This part was subjected to one test. Calculations based on a linear bending stress distribution and the loads applied in the tests indicated that no yielding occurred in the sections from where the specimens used in this work were extracted.

Test Data

The dimensions of smooth and notched specimens used in this material model calibration effort are given in Appendix A. Figure 1 shows the test data generated in the laboratory in the form of force over the minimal initial cross-sectional area (A_o) vs. deflection curves. All tests were conducted on the same servo-hydraulic uniaxial testing machine. The tensile force F was measured via a load cell while the displacement Δ was always measured with an extensometer with a one-inch gage length. The prescribed displacement rates were constant within each test, but could vary between test groups, and this will be indicated when presenting the data.

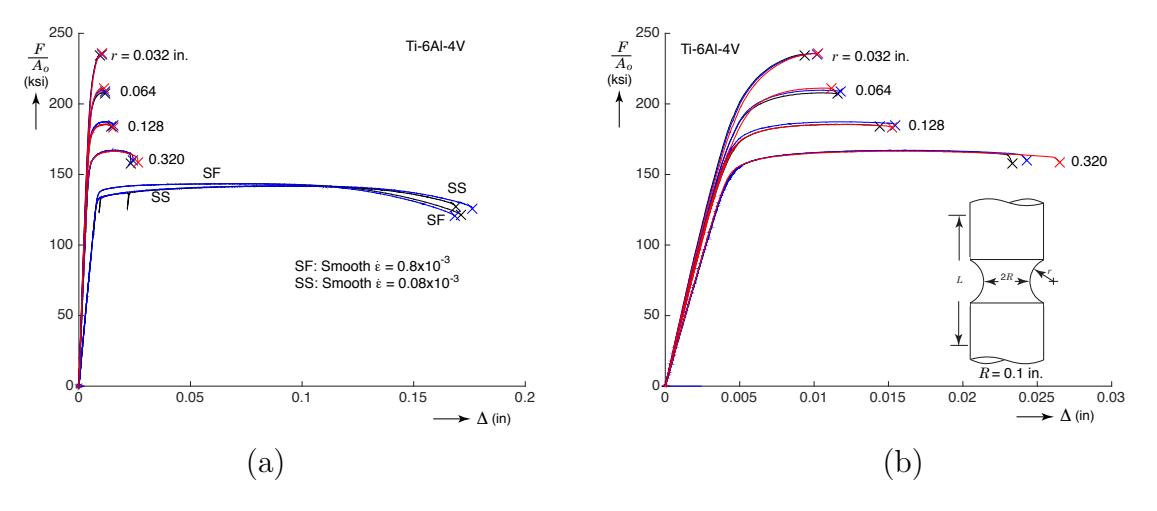


Figure 1. Test data. (a) All data and (b) notched tension tests only.

Four tests on smooth specimens were conducted as shown in Fig. 1(a) at two nominal strain rates ($\dot{\varepsilon}$). The strain rate for the curves labeled SS (for smooth slow) was 0.08×10^{-3} while for the curves labeled SF (for smooth fast) it was one order of magnitude faster. The response at each strain rate was repeatable, but some dependency on the strain rate is visible. The properties measured from these curves are given in Table 2. These properties include an estimate of the stress at the proportional limit σ_{pl} , where the linear relation between stress and strain ceases to be proportional. Comparison between the corresponding values shown in Tables 1 and 2 for the slow tests show that they are indeed very close.

Figure 1(b) shows a close-up of the measured response of the notched specimens. The prescribed stroke speed in all these tests was 0.05×10^{-3} in/s. All specimens had a diameter of 0.2 in. at their minimum cross-section and the notch radii are given in the figure. Three tests were carried out for each value of notch radius, and the measured responses were quite

Test	$\dot{arepsilon}$	E	σ_{pl}	σ_o	σ_u	ε_f
	(1/s)	(Msi)	(ksi)	(ksi)	(ksi)	
SS1	0.08×10^{-3}	16.73	123	133.8	141.7	0.169
SS2	0.08×10^{-3}	16.75	123	133.8	142.0	0.176
SF1	0.8×10^{-3}	16.75	126	138.6	143.5	0.171
SF2	0.8×10^{-3}	16.73	126	138.6	143.3	0.169

Table 2. Measured material properties for each smooth specimen.

repeatable. As expected the major differences occurred on the value of Δ at failure, but even these fell within a narrow range.

Calibration

The calibration procedure consisted of two steps: The first was to conduct an inverse analysis to determine the true stress-strain curve (or hardening function) for the material based on the smooth specimen data. The second was to use the calibrated curve plus the data from the notched specimens to calibrate ductile failure models.

Figures 2(a) and (b) show the results for the fit of the uniaxial material responses from the smooth specimens. Multilinear fits of the test data were obtained using an often-used script developed by Tim Shelton (1542) specifically for this purpose. Figure 2(a) shows the results of the fits for the curves from tests SS2 and SF1 using finite element models with selective deviatoric elements of unit aspect ratio and sizes of h = 0.01 and 0.02 inches. Figure 2(b) shows the corresponding hardening functions. Both figures demonstrate that the effect of changing the element size from 0.01 to 0.02 inches was mild. Appendix B shows the hardening functions in tabular form. Finally, Figure 2(c) shows the comparison between the predicted and measured responses of the notched specimens. At this point no failure was included in the predictions. The predicted responses were very close to the measured ones, and little difference could be seen between the predictions using the hardening functions from the slow or fast uniaxial tests.

Two failure models, Johnson-Cook and Wellman's tearing parameter, were fit using failure data from the smooth and the notched specimens. As in previous instances, the calibration was based on the minimization of the error function

$$e = \sum_{1}^{N} \left| \frac{\Delta^p - \Delta^t}{\Delta^t} \right|,\tag{1}$$

where Δ^p is the predicted failure displacement for a given test, Δ^t is the measured failure displacement for the same test and N is the total number of tests considered, which was five in the present calibration. A new capability being implemented in the Lamé library of material models for Sierra/SM involves the modularization of elastic-plastic models. The capability of particular interest here is that coupling different constitutive models with different choices of failure criteria (as long as plastic deformation is decoupled from damage) is allowed. This

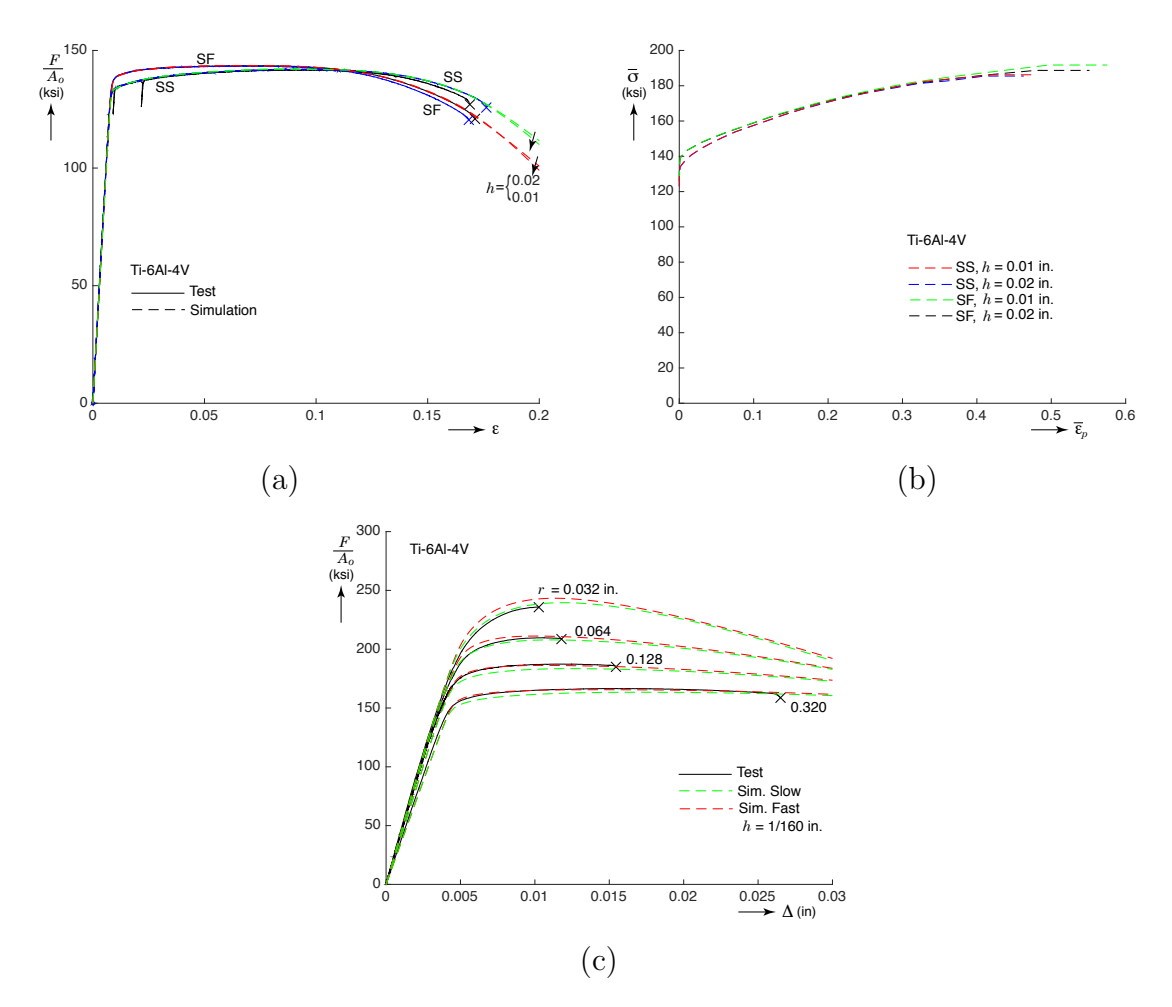


Figure 2. Results of fitting a piece-wise linear hardening function to a J_2 elastic-plastic model. (a) Comparison of measured and predicted engineering stress-strain curves, (b) hardening functions and (c) comparison of load-deflection predicted and measured responses for notched specimens.

new capability was exercised here by coupling the J_2 plasticity model with a multilinear fit of the hardening function and either the Johnson-Cook or the tearing parameter failure models.

Both failure models are triaxialy (η) dependent. Whereas the Johnson-Cook model is explicitly dependent on triaxiality, the tearing parameter is indirectly so. Both failure criteria depend on the integral of a stress-state-dependent expression through the loading history to calculate a damage parameter D. Initially D=0, but it grows as the material deforms plastically. The expressions for D are

$$D_{\rm jc} = \int \frac{d\bar{\varepsilon}_p}{d_1 + d_2 e^{d_3 \eta}} \tag{2}$$

for the Johnson-Cook failure model, where d_1, d_2, d_3 are the parameters to be determined from calibration and

$$D_{\rm tp} = \frac{1}{t_p} \int \left\langle \frac{2\sigma_{\rm max}}{3(\sigma_{\rm max} - \sigma_m)} \right\rangle^m d\bar{\varepsilon}_p \tag{3}$$

for the tearing parameter model where σ_{max} is the maximum principal stress, σ_m is the hydrostatic stress and t_p and the exponent m are the model parameters to be determined. In both cases, material failure is taken to occur when D=1.

The calibration consisted of first simulating all tests using models with selective deviatoric elements of size 1/160 inches. All parameters needed to evaluate both failure criteria were averaged over each element and output to file for the critical elements where failure was likely. Subsequently, the error function e was evaluated in a Matlab script by varying the values of the model parameters in discrete steps. The parameters d_3 and m varied in increments of one, d_2 and t_p in increments of 0.01 and d_1 in increments of 0.025 (see Appendix C for examples of the calibration procedure). Both strain rates in the uniaxial tension tests were considered. The minimum values of e occurred when the fit for the slower strain rate was used in the calculations. The parameters chosen are given in Table 3.

Table 3. Results for failure calibration.

Johnson-Cook		Tearing Parameter		
d_1	d_2	d_3	t_p	m
0.025	1.67	-3	0.81	4

Figure 3 shows the results of the calibration for both failure models. Figures 3(a) and (c) show the comparison of the measured failure points in the tests and those predicted by the two failure criteria in simulations. The agreements seem reasonably good. Figures 3(b) and (d) show the same comparisons in the plastic-strain vs. triaxiality space. In all cases but the ones with R=0.032 in., the models predicted failure at the center of the narrowest cross-section of the specimens. When R=0.032 in., both models predicted failure at 3/4 of the radius from the center, also at the narrowest cross-sections.

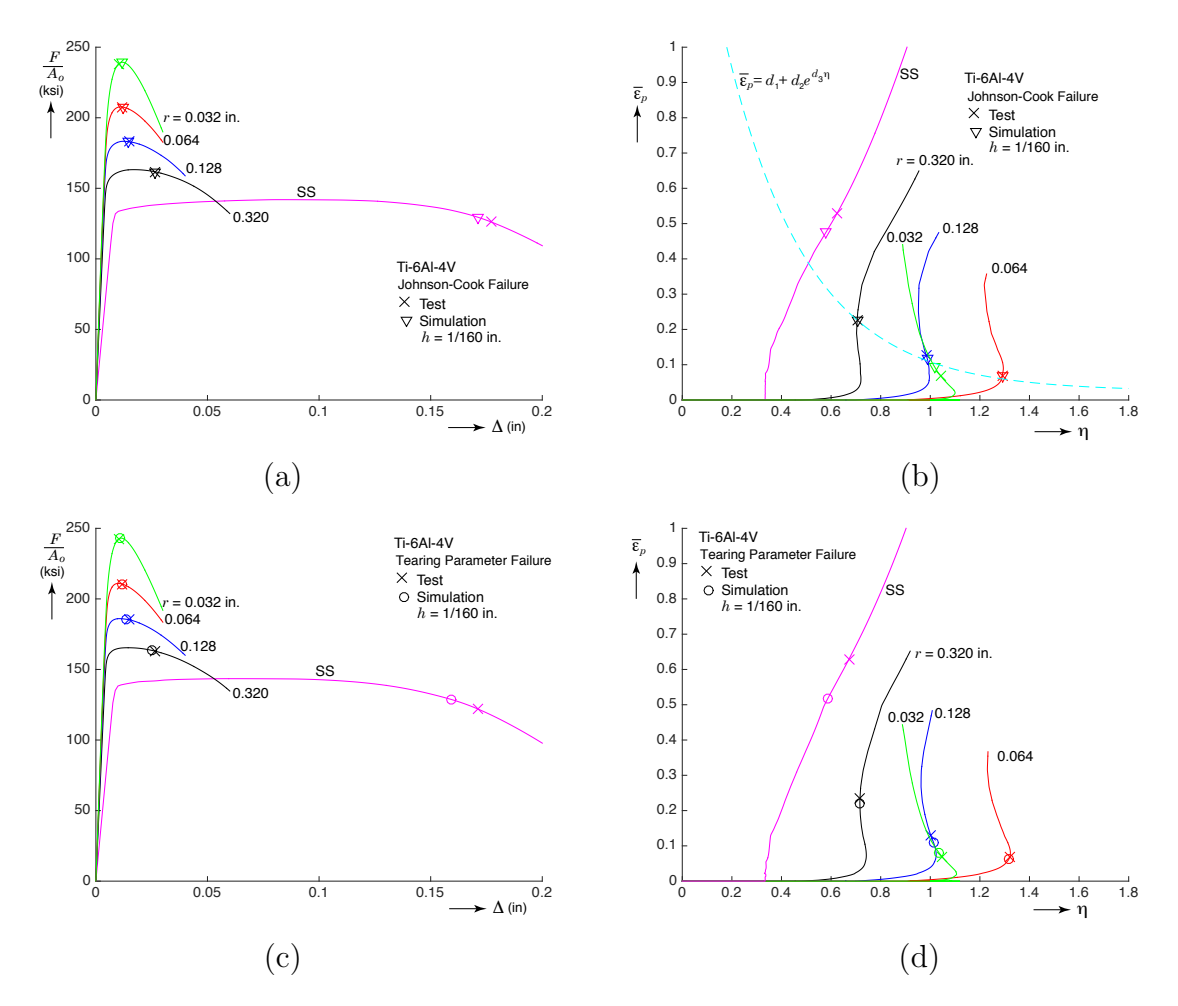


Figure 3. Results of the failure model calibrations. (a) Comparison of displacements at failure for Johnson-Cook, (b) comparison of points at failure in plastic-strain vs. triaxiality space for Johnson-Cook, (c) comparison of displacements at failure for tearing parameter and (d) comparison of points at failure in plastic-strain vs. triaxiality space for tearing parameter.

The calibration schemes were verified by simulating all the tests with the optimal parameters for the failure criteria, and comparing the values of Δ at which the models predicted failure to the corresponding results from the calibration procedure. The agreement was excellent in all cases.

An exercise was then conducted to briefly explore the effect of element size and type on the failure predictions. This consisted running simulations of all tests using the hardening function corresponding to the slow strain rate and the failure parameters in Table 3, but using elements with h=1/80 inches of both the selective deviatoric and uniform gradient kinds. Table 4 displays the percentage difference obtained with the larger elements. Note that in all cases the difference was positive, indicating larger displacements to failure for the larger elements. Using the uniform gradient elements caused the most deviation. Given that failure simulations tend to have large uncertainties, the differences seen in the table are not too concerning at this time, but they indicate that failure predictions can be sensitive to both element size and type, so proper care must be exercised when using the calibrations in other situations.

Table 4. Percent increse of Δ at failure between cases run with selective deviatoric (SD) and uniform gradient (UG) elements with h = 1/80 inches when compared with the results with SD elements with h = 1/160 inches.

Element	Smooth	R = 0.320	0.128	0.064	0.032
SD	0.4	2.2	4.2	3.8	1.2
UG	3.6	9.0	8.4	2.8	2.5

Summary

Calibrations of the hardening function of Ti-6Al-4V alloy for J_2 plasticity models as well as of failure models were carried out and are provided in this report. Tensile tests on smooth and notched specimens provided the data needed for the calibration. The applicability of this calibration is for tensile-dominated states of stress. The high values for the parameters d_3 and m that resulted from the calibration will suggest very high values of equivalent plastic strain at failure for shear-dominated states of stress with triaxiality in the vicinity of zero. No test data is currently available for establishing what the plastic strain at failure would be at low triaxiality values.

Acknowledgments

Thanks go to the staff in Org. 1528 who helped generate the test data used in this work. Specifically, Jack Heister assisted with specimen design and manufacturing while Kim Haulenbeek and Dave Johnson conducted the tests. Nicole Breivik, Doug VanGoethem and Mike Guthrie participated in several discussions that motivated this work.

Sandia National Laboratories is a multimission laboratory managed and operated by National Technology and Engineering Solutions of Sandia, LLC, a wholly owned subsidiary of Honeywell International, Inc., for the U.S. Department of Energy's National Nuclear Security Administration under contract DE-NA0003525.

Appendix A

Figures 4 to 8 show the dimensions of the five types of specimens used.

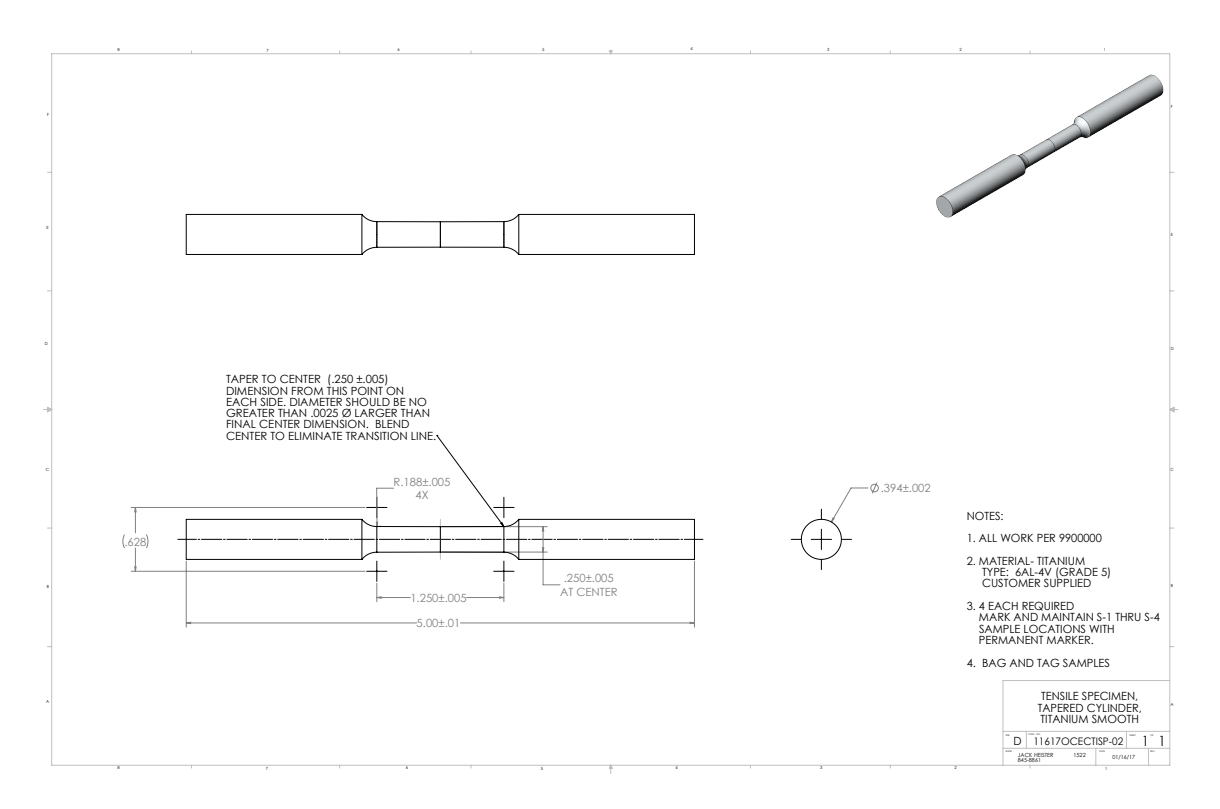


Figure 4. Smooth specimen.

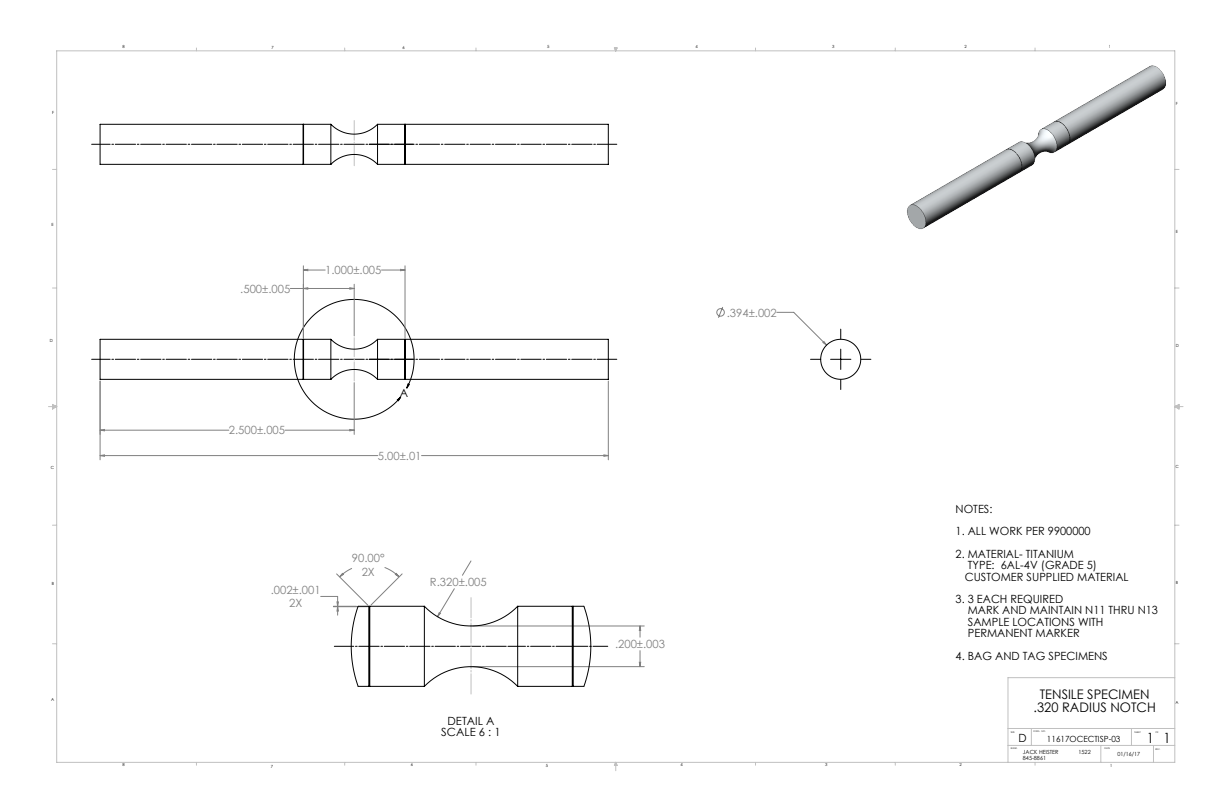


Figure 5. Notched specimen, R = 0.320 in.

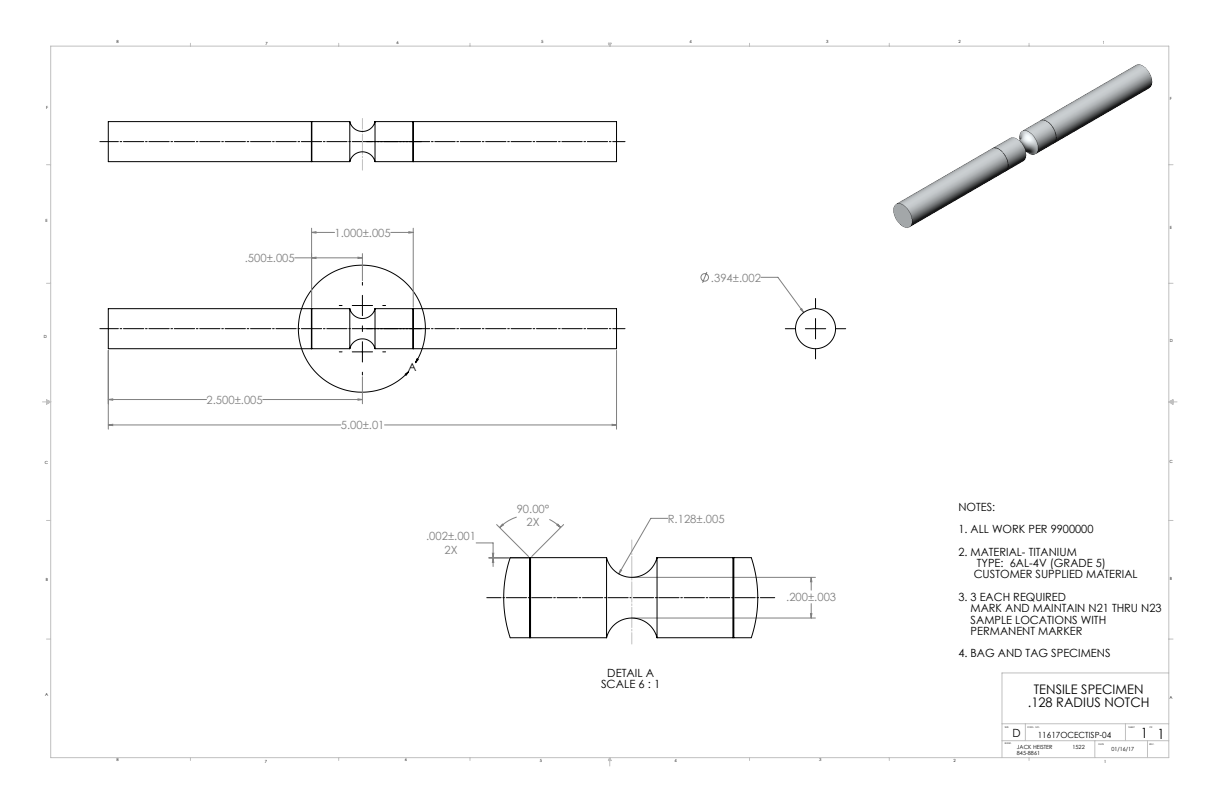


Figure 6. Notched specimen, R = 0.128 in.

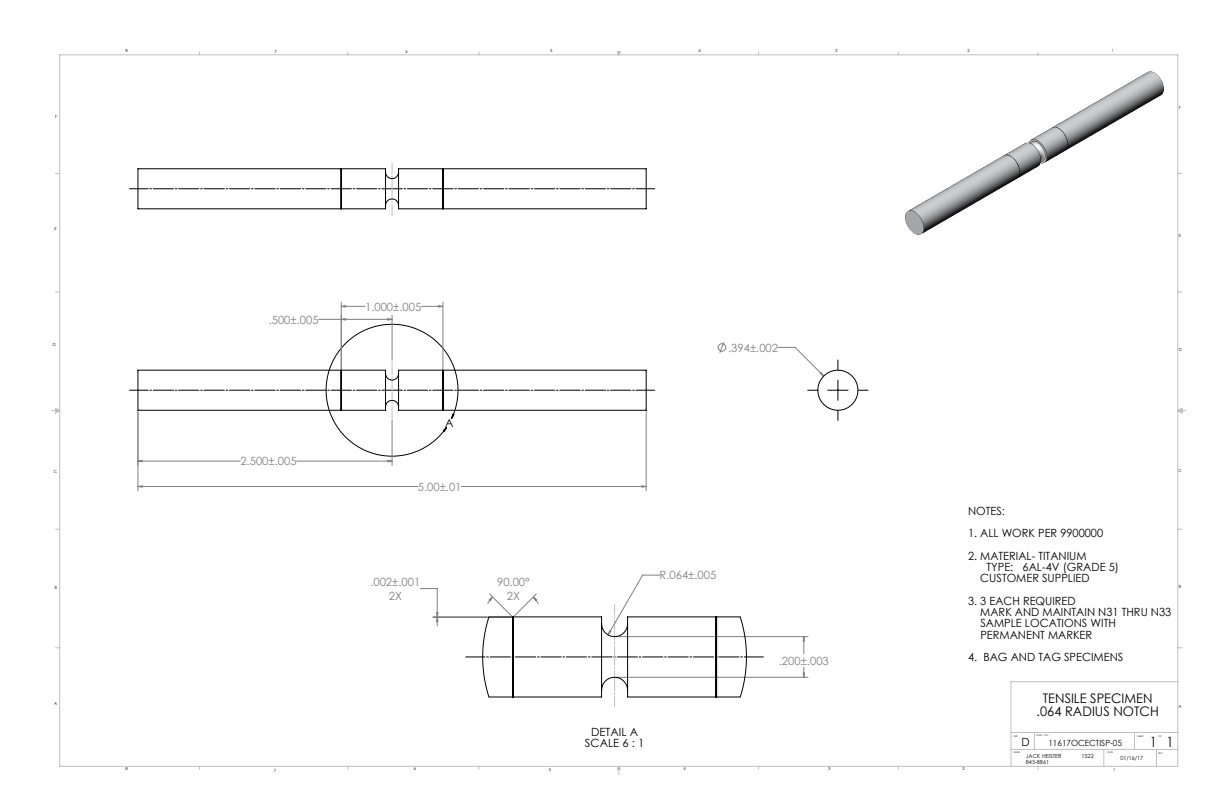


Figure 7. Notched specimen, R = 0.064 in.

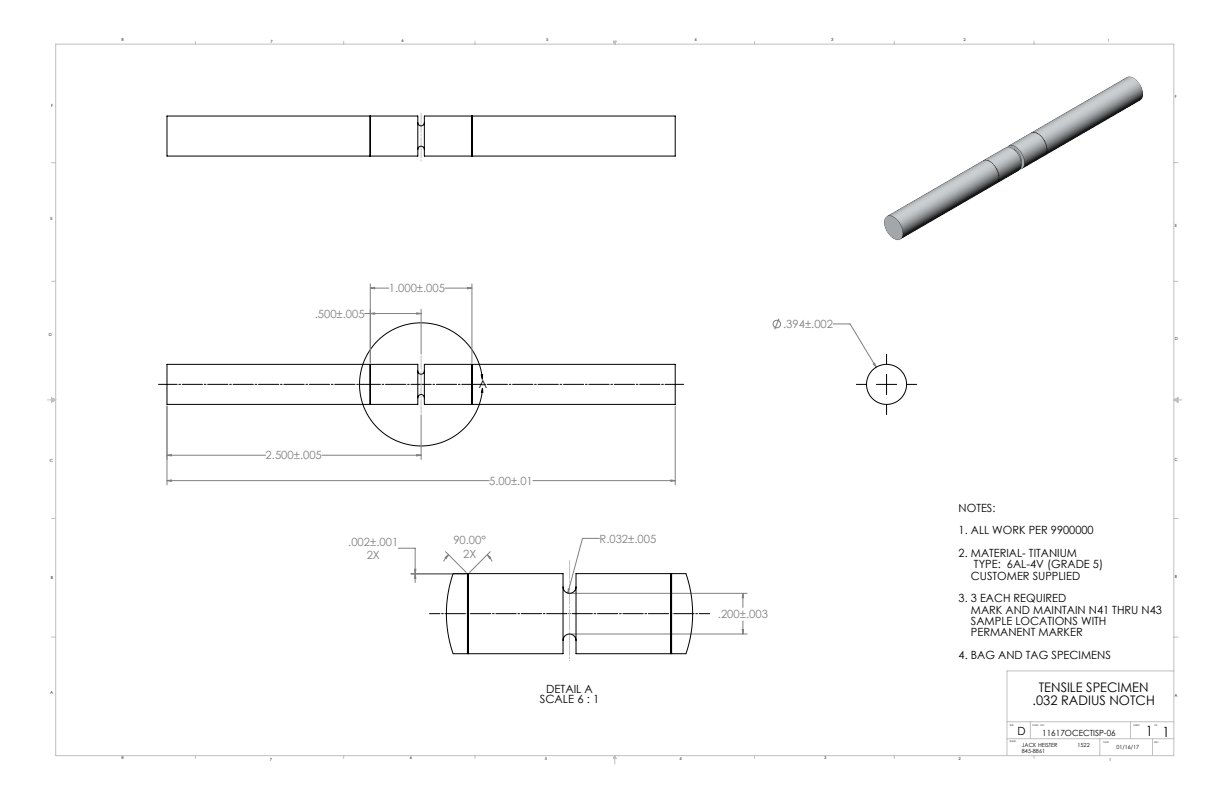


Figure 8. Notched specimen, R = 0.032 in.

Appendix B

The hardening function obtained from the slow strain rate uniaxial tension test using selective deviatoric elements with h = 0.01 inches was as follows:

```
begin definition for function hardening
type is piecewise linear
begin values
  0.0, 123000.0
   0.000257354909125, 129700.832321
   0.00105735549017, 133844.793188
   0.00258914361261, 134836.615911
   0.00782374031699, 137584.703542
  0.015935624467, 140693.00005
   0.0245506692978, 143122.981944
   0.0327440436203, 145206.836272
  0.041103022862, 147138.528138
   0.0498559397622, 148958.712962
  0.0577172078918, 150593.477819
  0.0667430676139, 152293.041188
  0.075415743371, 153926.100251
   0.0905101163251, 156160.037189
   0.10763956847, 158695.161767
   0.124440820301, 161181.713358
  0.14199919078, 163780.31699
   0.163969140995, 166600.963036
  0.188526790223, 169753.834824
   0.217847017572, 172679.907571
   0.250302928467, 175918.912346
   0.286428946175, 178951.856275
   0.325661143559, 182245.578152
  0.370565509704, 184130.541308
   0.420194143788, 186213.816382
   0.47700502647, 186213.816382
  3.00000000000, 186213.816382
end values
end definition for function hardening
```

The hardening function for the fast strain rate uniaxial tension test was

```
begin definition for function hardening type is piecewise linear
```

```
begin values
   0.0, 126000.0
   9.41853487797e-05, 132310.418368
   0.000813054948367, 137622.749311
   0.00185011030942, 139538.667472
  0.00581451234925, 141369.685889
   0.0115110697479, 143703.14734
   0.0205413698649, 145552.672915
  0.0229555777484, 146541.596687
   0.0313518992086, 148261.275001
   0.0400437922174, 149784.501681
   0.0473987220843, 151073.429812
   0.0542439856316, 152273.040536
   0.0635642258642, 153654.718024
   0.0745169790247, 155278.407125
  0.0860922029488, 156994.374302
   0.105941498775, 159936.929914
   0.126899575016, 163043.856498
   0.154249141109, 166515.299908
   0.186974621885, 170310.040097
   0.224181361465, 174288.125813
   0.266431157435, 178200.875923
   0.314289382777, 181923.355297
   0.368465670622, 185254.508712
   0.429332908313, 188332.478898
   0.496675393069, 191737.893176
   0.575088238128, 191737.893176
   3.00000000000, 191737.893176
end values
end definition for function hardening
```

The J_2 plasticity model input with Johnson-Cook failure model for the slow strain rate fit was as follows (note a Poisson ratio value of 0.32 was used instead of the value of 0.31 listed in the MMPDS-08):

```
begin property specification for material mat_1
  density = 1.0
  begin parameters for model j2_plasticity
    youngs modulus = 16.75e6
    poissons ratio = 0.32
    yield stress = 123000.
    hardening model = user_defined
    hardening function = hardening
```

```
failure model = johnson_cook_failure
  johnson_cook_d1 = 0.025
  johnson_cook_d2 = 1.67
  johnson_cook_d3 = -3.0
  johnson_cook_d4 = 0. ### No rate dependence ###
  johnson_cook_d5 = 0. ### No temperature dependence ###
  reference rate = 1.e-6 ### Unused, no rate dependence ###
  critical failure parameter = 1.0
  critical crack opening strain = 1.e-16 ### Not calibrated ###
  end parameters for model j2_plasticity
end property specification for material mat_1
```

The J_2 plasticity model input with tearing parameter failure model and the slow strain rate fit was as follows:

```
begin property specification for material mat_1
  density = 1.0
  begin parameters for model j2_plasticity
    youngs modulus = 16.75e6
    poissons ratio = 0.32
    yield stress = 123000.
    hardening model = user_defined
    hardening function = hardening
    failure model = tearing_parameter
    tearing parameter exponent = 4
    critical failure parameter = 0.81
    critical crack opening strain = 1.e-16  ### Not calibrated ###
  end parameters for model j2_plasticity
end property specification for material mat_1
```

Appendix C: Examples of Selection of Failure Parameters

This appendix presents examples of the procedures used to select the parameters suggested in Table 3. Figure 9 shows an example for tearing parameter. Figure 9(a) shows the variation of e (Eqn. 1) as t_p changes, for four values of m. In each case, the optimal t_p is the value that minimizes e and then the optimal m is the one that gives the lowest minimum. Figure 9(b) shows the failure displacements for each combination of t_p and m. Note that the variation in the predicted failure displacement was much larger for the smooth specimen than the notched ones.

Figure 10 shows a similar example for the Johnson-Cook model. Since this model has three parameters vs. two for the tearing parameter, the effort was somewhat larger. Figure 10(a)

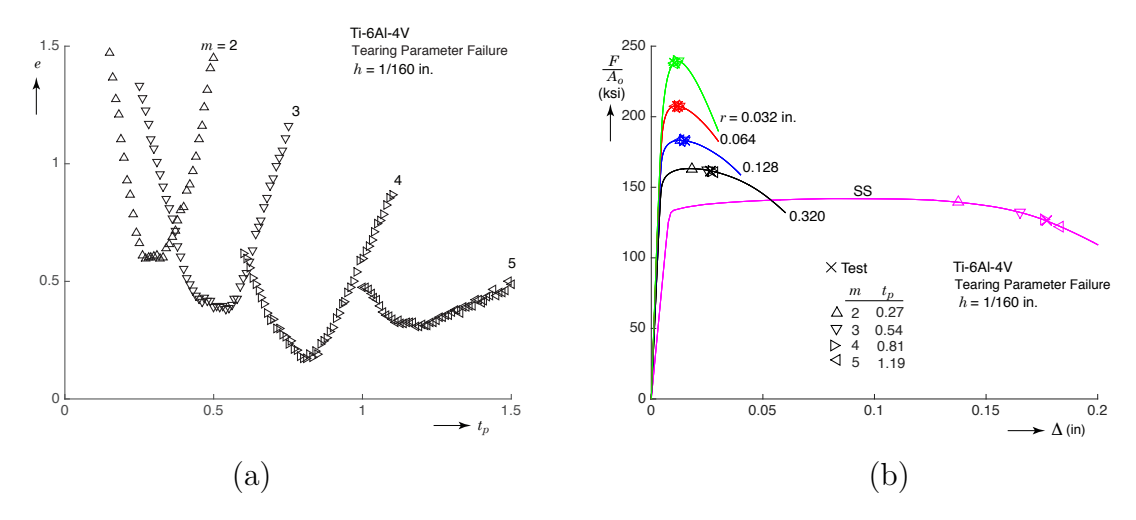


Figure 9. Example of selection of tearing parameters m and t_p . (a) Error e as function of t_p for different values of m and (b) comparison of measured and predicted failure displacements for the value of t_p that minimized e for each value of m.

shows how e varies as d_2 changes for four values of d_3 while d_1 was fixed at the value indicated. As before, the combination chosen was the one that gave the minimum e. Figure 10(b) shows the failure displacements for each combination of d_2 and d_3 .

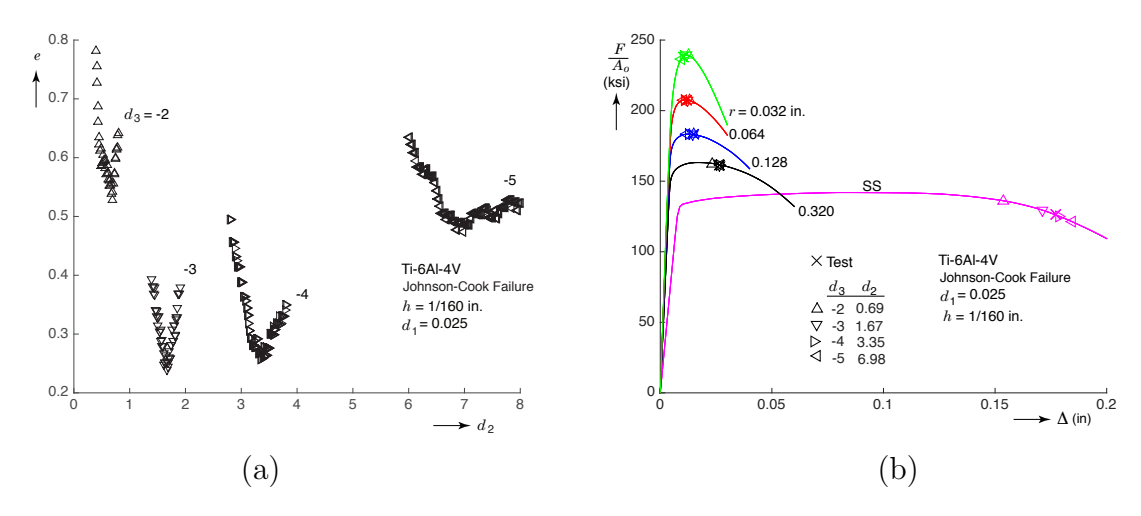


Figure 10. Example of selection of Johnson-Cook parameters d_2 and d_3 for $d_1 = 0.025$.

(a) Error e as function of d_2 for different values of d_3 and (b) comparison of measured and predicted failure displacements for the value of d_2 that minimized e for each value of d_3 .

Figure 11 shows the failure results obtained for each optimal combination of d_2 and d_3 for three values of d_1 . Since d_1 represents the floor of the strain to failure (see Eqn. 2) higher values of d_1 seem unlikely.

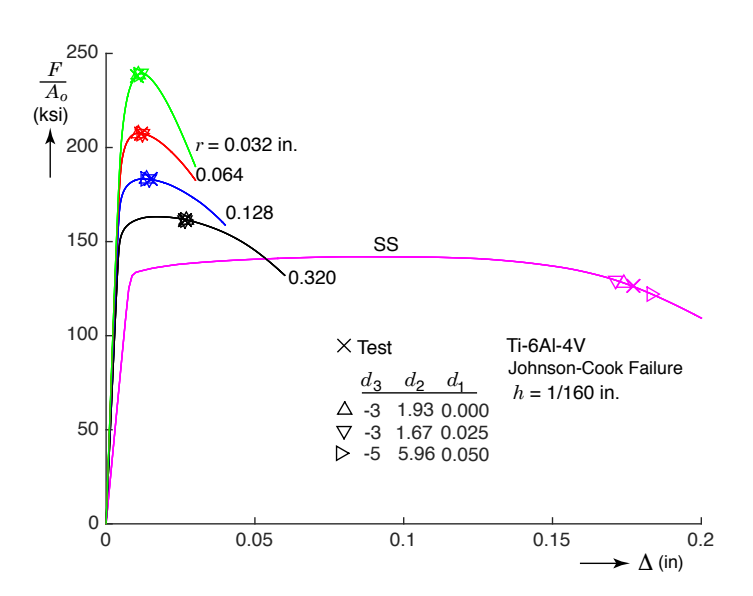


Figure 11. Comparison of measured and predicted failure displacements for the values of d_2 , d_3 that minimized e for three values of d_1 .

Internal Distribution:

K. Haulenbeek	1528
M. Guthrie	1553
E. Fang	1554
W. Scherzinger	1554
D. VanGoethem	1554